

**METABOLIC STRESS CONTROL OF CYTOSKELETAL DYNAMICS AND
METASTASIS**

M. Cecilia Caino, Young Chan Chae, Valentina Vaira, Stefano Ferrero, Mario Nosotti,
Nina M. Martin, Ashani Weeraratna, Michael O’Connell, Danielle Jerningan, Alessandro Fatatis,
Lucia R. Languino, Silvano Bosari, and Dario C. Altieri

SUPPLEMENTAL INFORMATION

Table of contents:

Supplemental Materials and Methods

Supplemental Tables 1-2

Supplemental Figures 1-8

Supplemental References

SUPPLEMENTAL MATERIALS AND METHODS

Antibodies and reagents. The following antibodies to Ser473-phosphorylated Akt (Cell Signaling), Akt (Cell Signaling), Thr202/Tyr204-phosphorylated ERK1/2 (Cell Signaling), ERK1/2 (Cell Signaling), Tyr397-phosphorylated FAK (Invitrogen), Tyr925-phosphorylated FAK (Cell Signaling), FAK (Cell Signaling), Tyr416-phosphorylated Src (Cell Signaling), Src (Cell Signaling), Rac1 (Upstate), Cdc42 (Cell Signaling), Ser199/204-phosphorylated Pak1/Ser192/197-phosphorylated Pak2 (Cell Signaling), Ser144-phosphorylated Pak1/Ser141-phosphorylated Pak2 (Cell Signaling), Ser20-phosphorylated Pak2 (Cell Signaling), Pak1/2/3 (Cell Signaling), FIP200 (Novus Biologicals), TRAP-1 (BD Biosciences), HA (Roche), LKB1 (Cell Signaling), Thr172-phosphorylated AMPK α (Cell Signaling), AMPK α (Cell Signaling), *atg5* (Cell Signaling), Ser792-phosphorylated Raptor (Cell Signaling), Raptor (Cell Signaling), Ser2448-phosphorylated mTOR (Cell Signaling), mTOR (Cell Signaling), Thr37/46-phosphorylated 4EBP1 (Cell Signaling), 4EBP1 (Cell Signaling), Ser79-phosphorylated Acetyl-CoA Carboxylase (ACC) (Cell Signaling), ACC (Cell Signaling), Ser555-phosphorylated ULK1 (Cell Signaling), Ser757-phosphorylated ULK1 (Cell Signaling), ULK1 (Santa Cruz), LC-3 (Cell Signaling), pan-phosphorylated-Ser residues (Millipore), β -tubulin (Sigma-Aldrich) and β -actin (Sigma-Aldrich) were used.

The plasmids encoding Cdc42^{V12} (Addgene #11399), Rac1^{V12} (Addgene #11397), HA-tagged FIP200 (Addgene #24303), myc-tagged wild type ULK1 (Addgene #27629), myc-tagged kinase inactive (KI) ULK1 (Addgene #27630), myc-tagged ULK1 non-phosphorylatable mutant 4SA (Addgene #27631), constitutively activated AMPK α 1 (AMPK^{CA}, 1-312) (Addgene #27632), Src (Addgene #13663) were used. A cDNA encoding FAK or TRAP-1 was cloned into pcDNA6/myc-His (Invitrogen), and the construct was validated by DNA sequencing.

The complete chemical synthesis, HPLC profile, and mass spectrometry of mitochondrial-targeted small molecule Hsp90 antagonist, Gamitrinib (GA mitochondrial matrix inhibitors) has been reported previously (1). The Gamitrinib variant containing triphenylphosphonium as a mitochondrial-targeting moiety was used in this study (1). Non-mitochondrially permeable Hsp90 inhibitor 17-allylamino demethoxygeldanamycin (17-AAG) was obtained from LC-Laboratories. 2-deoxy-D-glucose (2-DG) and carbonyl cyanide 3-chlorophenylhydrazone (CCCP) were obtained from Sigma-Aldrich. Rapamycin and metformin were obtained from EMD. Calcein-AM and Topro were from Invitrogen.

Transfections. Gene knockdown experiments were carried out using control, non-targeting small interfering RNA (siRNA) pool (Dharmacon, cat. no. D-001810) or specific siRNA pools targeting TRAP-1 (Dharmacon, cat. no. L-010104), *atg5* (Dharmacon, cat. no. L-004374), LKB1 (Dharmacon, cat. no. L-005035), AMPK α 1/ α 2 (Santa Cruz Biotechnology, cat. no. sc-45312), FIP200 (Dharmacon, cat. no. L-021117), or ULK1 (Santa Cruz Biotechnology, cat. no. sc-44182). Individual ON-Target SMART siRNA were used for TRAP1 (Dharmacon, cat. no. J-010104-05, -06, -07 and -08), LKB1 (Dharmacon, cat. no. J-005035-07, -08, -09 and -10), AMPK α 1/ α 2 (Santa Cruz Biotechnology, cat. no. sc-45312A, B and C), and FIP200 (Dharmacon, cat. no. J-021117-05, -06, -07 and -08).

For gene silencing, pooled or individual siRNA oligonucleotide sequences were transfected at 10-30 nM concentrations in the presence of Lipofectamine RNAiMAX in a 1:1 ratio (Invitrogen). Cells were incubated for 48 h, validated for target protein knockdown by Western blotting, and processed for subsequent experiments. Plasmid DNA transfections were carried out using X-tremeGENE HP DNA transfection reagent (Roche) for PC3 or LN229 cells, or Lipofectamine LTX (Invitrogen) for MDA-231, NIH3T3 or H460 cells. In some experiments,

LN229 or PC3 cells were transfected with siRNA directed to human ULK1, incubated for 48 h, and subsequently transfected with siRNA-resistant mouse ULK1 cDNA constructs.

Cell migration and invasion. Various tumor cell types were treated as indicated in each experiment, suspended in 0.1% BSA/DMEM and seeded ($1.6\text{-}3.2 \times 10^3$ cells/mm², depending on the cell type) in the upper compartment of 8 μM pore diameter BD transwells (BD). NIH3T3 conditioned medium was placed in the lower compartment as a chemoattractant. After 6-18 h incubations at 37°C, the transwell membranes were recovered and cells on the upper side (non-migratory) were wiped off the surface. Cells on the lower side of the membrane were fixed in methanol, rinsed in water and mounted on glass slides with Vectashield medium containing DAPI (Vector Laboratories). Migrated cells on each membrane were counted by fluorescence microscopy in 5 different fields. For cell invasion assays, transwell membranes were coated with Matrigel and processed as described above.

For cell migration experiments using a wound closure assay, confluent monolayers of MRC-5 cells were incubated with vehicle or Gamitrinib (5-10 μM), and wounded using a 10 μl pipette tip. Three micrographs/well were obtained at time=0, 16 and 24 h after wounding, and the percentage of wound closure was normalized to the maximum initial area for each well.

For analysis of tumor cell invasion in 3D organotypic spheroids, tumor cells (5×10^4) were seeded onto 96-well plates coated with 1.5% agar (Difco Noble Agar) in PBS, pH 7.4. Spheroids were allowed to form over a 72 h period and then embedded in 600 μl of bovine collagen type I (Organogenesis) in 24-well plates. Spheroids were overlaid with 1 ml of growth medium, treated with various concentrations of Gamitrinib for 72 h, and analyzed for changes in maximum invasion distance and invasion area. Quantification of live vs. dead cells under the various conditions tested was performed by staining the spheroids with calcein-AM (live, *green*) and

Topro-3 (dead, *blue*) (Invitrogen) for 2 h. Samples were imaged using a Prairie Ultima II 2-photon microscope (Prairie Technologies, Inc, Middleton, WI), and stacks of 100 slices were generated in 2 channels. 3-D reconstruction of the labeled spheroids and analysis of cell staining was carried out using ImagePro Plus 3D software (Media Cybernetics, Silver Spring Maryland).

For analysis of nutrient deprivation, tumor cell types were preincubated in the presence of 50% amino acids or 5 mM glucose for 16 h before seeding for cell migration or cell invasion studies. BSA (0.1%) or dialyzed FBS (10%) were added to the upper and lower compartments of the Transwell chamber, respectively, to maintain the nutrient-deprived conditions throughout the cell motility studies.

Rac1 and Cdc42-GTP pull-down assays. The activation of Rho family small GTPases, Rac1 or Cdc42 was examined in pull-down assays using the p21-binding domain (PBD, amino acids 70-117) of the p21-activated kinase-1 (Pak1). Briefly, a pGEX TK-Pak1 PBD cDNA (Addgene, Cat. no. #12217) was purified, transformed into BL21 *E.coli* competent cells (Stratagene), and expressed as recombinant GST fusion protein after induction with 1 mM IPTG for 4 h at 34°C. Cells were suspended in PBS, pH 7.2, in the presence of protease inhibitors (SIGMA), and broken by sonication in 1% Triton X-100 for 30 min at 4°C. Soluble proteins were isolated by chromatography on glutathione Sepharose 4B (GS4B, GE Healthcare), eluted in 3 consecutive steps in buffer containing 10 mM GSH, 50 mM Tris HCl, pH 8.0, and further desalted using Amicon Ultra 4/10K columns (Millipore), for a total of 3 buffer changes to PBS, pH 7.2. The protein was diluted in glycerol, quantified by absorbance at 280 nm, and stored at -80°C until use. The activity of each batch of recombinant protein was assessed by incubating aliquots of the cell lysate with non-hydrolyzable GTP γ S at 0.1 mM (maximum binding) or 1 mM GDP (negative control) in low Mg²⁺ buffer at 30°C followed by pull-down(2).

For modulation of small GTPase activity, tumor cells at 30% confluency were serum-starved for 48 h, stimulated with FBS (10% for 5 min) or EGF (100 ng/ml for 2 min), and lysed in pull-down buffer containing 20 mM Tris-HCl, pH 7.4, 150 mM NaCl, 5 mM MgCl₂, 0.5% NP-40, 5 mM β-glycerophosphate, 1 mM DTT plus protease inhibitors in the presence of 15 μg/ml of GST-Pak1 PBD. Lysates were cleared by centrifugation at 13,000 g for 10 min at 4°C, and incubated with GS4B beads for additional 45 min at 4°C. After centrifugation, GS4B-bound proteins were washed twice in pull-down buffer, separated by electrophoresis on SDS polyacrylamide gels, and Rac1 and Cdc42 levels in pellets or whole cell lysates were analyzed by Western blotting.

F-actin staining. Tumor cells growing at low confluency ($1-2 \times 10^4$ /well) on optical grade glass coverslips were treated with vehicle or Gamitrinib (5 μM), fixed in 4% formaldehyde for 15 min at 37°C, washed in PBS, pH 7.4, and permeabilized with 0.1% Triton X-100 for 5 min at 22°C. Slides were washed in PBS, pH 7.4, blocked in 1% BSA/PBS for 30 min, incubated with 1:2000 dilution of phalloidin-rhodamine (Molecular Probes) for 30 min, washed in PBS, pH 7.4, and mounted in Fluoromount G medium (Southern Biotech). Slides were analyzed on a Leica TCS SP2 confocal laser microscope with a 100X oil objective.

Quantification of lamella dynamics in live cells. Tumor cells growing at low confluency ($3-5 \times 10^4$ /well) on high optical quality 96 well μ-plates (Ibidi) were imaged with a 40X objective on a Nikon TE300 inverted time-lapse microscope equipped with a video system containing a Evolution QEi camera and a time-lapse video cassette recorder. All experiments were carried out in atmosphere-equilibrated environment at 37°C and 5% CO₂. Phase contrast images were captured at 0.5 sec intervals for 5 min (600 images=300 sec) and merged into sequence files using ImagePro Plus 7. Real time dynamics of a particular cellular region were quantified by

Stroboscopic Analysis of Cell Dynamics (SACED) (3), with generation of digital steps from the first 120 sec (240 frames) of the sequence files imported into Image J software. A particular region of 16.2 μm x 0.162 μm (“SACED line”) was selected in cells under analysis, duplicated and montaged in sequence to display the region over time in a stroboscopic image. This process was repeated to obtain a total of 4 SACED lines and therefore 4 stroboscopic images per each cell, which were separately displayed to quantify lamella dynamics. Structures such as protruding lamellipodia and ruffles were manually labeled and the frequency of ruffles per min was calculated. Mean values were calculated from at least 15 cells from 4 separate wells. All experiments were repeated at least twice with different tumor cell types.

Detection of FIP200 phosphoisotypes. Analysis of phosphoisotypes was carried out by standard phosphate-affinity SDS gel electrophoresis, using a mobility shift protocol (4). Briefly, proteins were separated by electrophoresis on 3% polyacrylamide/0.5% SeaKem Gold Agarose (Lonza) gels containing the dinuclear metal complex Mn^{2+} -Phos-tag (Acrylamide-pendant Phos-tag, Wako Chemicals). After removal of Mn^{2+} by washing the gels in blotting buffer containing 1 mM EDTA, proteins were transferred to PVDF membranes and detected by Western blotting using antibodies to FIP200 or pan-phosphorylated Ser residues. In some experiments, FIP200 immune complexes precipitated from Gamitrinib-treated PC3 cells were treated in the presence or absence of alkaline phosphatase (20,000 U) for 1 h at 37°C followed by Western blotting using antibodies to FIP200 or pan-phosphorylated Ser residues.

Cell viability and cell proliferation assays. Tumor cells were plated onto 96-well plates at 3.7×10^3 /well and treated with vehicle or Gamitrinib (5 μM). After 24 h, cell viability was assessed with a 3-(4,5-dimethyl-thiazoyl-2-yl)-2,5-diphenyltetrazolium bromide (MTT) colorimetric assay (1), or, alternatively, by Trypan blue exclusion and light microscopy. Data

were background-subtracted relative to vehicle-treated cultures. In some experiments, tumor cell proliferation was assessed by direct cell counting and light microscopy.

Tissue microarray (TMA). Representative tissue blocks from patients affected by NSCLC were used to build seven TMAs (NSCLC-TMA), as described previously(5). For each patient, four cores of neoplasia were included in the blocks as well as 34 cores of non-neoplastic lung parenchyma. For quality control, a 4- μ m-thick section was cut from each TMA block, stained with H&E, and analyzed by immunohistochemistry.

Immunohistochemistry. NSCLC-TMA slides were subject to antigen retrieval in EDTA solution. Sections (4- μ m thick) were cut from all TMA blocks and stained with a rabbit monoclonal antibody to phospho-ULK1 Ser555 (1:500, clone D1H4), or to phospho-ULK1 Ser757 (1:100) overnight at 4°C or for 30 min at 22°C, respectively. Immunohistochemistry (IHC) was performed using a Ventana BenchMark Ultra autostainer (Ventana Medical Systems), with the ultraView Universal DAB Detection Kit (Ventana) for detection of antibody reactivity. All slides were counterstained with hematoxylin. Immunoreactivity for the various markers was evaluated by two pathologists (S.F. and S.B.) and independently scored for cytoplasmic or nuclear localization. The percentage of immunoreactive epithelial cells was recorded and when discrepancies in scoring occurred, a consensus interpretation was reached after re-examination. Among the lung AdCa samples in the series under investigation, 20 cases were negative for Ser555 expression, whereas 15 cases of SCC were Ser555-negative. The ULK1-Ser757 immunoreactivity was detected in both cytoplasm and nuclei. The number of immunoreactive or negative cases per phospho-ULK1 protein is summarized in Supplemental Table 2. Ninety-two AdCa and 37 SCC patients could be analyzed for both S555 and S757 immunoreactivity.

Supplemental Table S1. Characteristics of NSCLC patients examined in this study.

	Clinico-pathological feature	Histotype	
		AdCa (n=123)	SCC (n=57)
Gender	Male	91	50
	Female	33	7
Age	Median (range)	62.5 (42-78)	65.6 (45-82)
Grade (G)¹	G1	5	1
	G2	52	23
	G3	51	26
Tumor size (T)	T1a	18	7
	T1b	14	7
	T2a	50	23
	T2b	10	8
	T3	28	10
	T4	3	2
Lymph node metastases (N)	Nx	6	-
	N0	65	35
	N1	27	19
	N2	25	3
	N3	-	-
Distant metastases (M)	M1a	5	2
Status	Alive	55	22

¹ Grade was not available for 15 AdCa and 7 SCC cases

	Dead	68	35
--	------	----	----

Supplemental Table S2. Immunoreactivity of ULK1-Ser555 and ULK1-Ser757 detected in NSCLC patients.

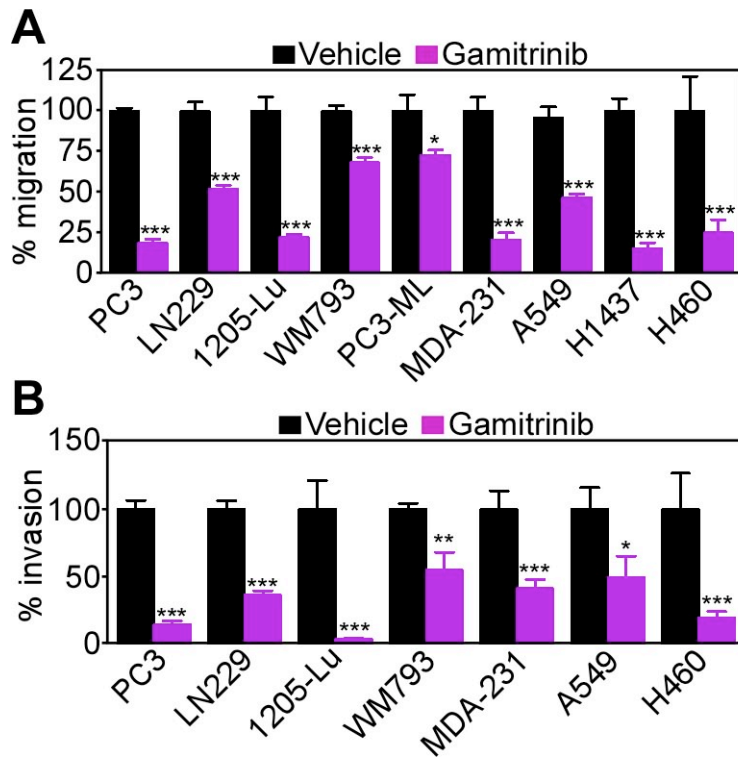
Antibody	Localization	NSCLC histotype	Positive IHC	Negative IHC
Ser555 ²	Nuclear	AdCa	98	20
		SCC	40	15
Ser757 ³	Nuclear	AdCa	74	49
		SCC	2	55
	Cytosolic	AdCa	38	83
		SCC	5	52

AdCa, adenocarcinoma; SCC, squamous cell carcinoma.

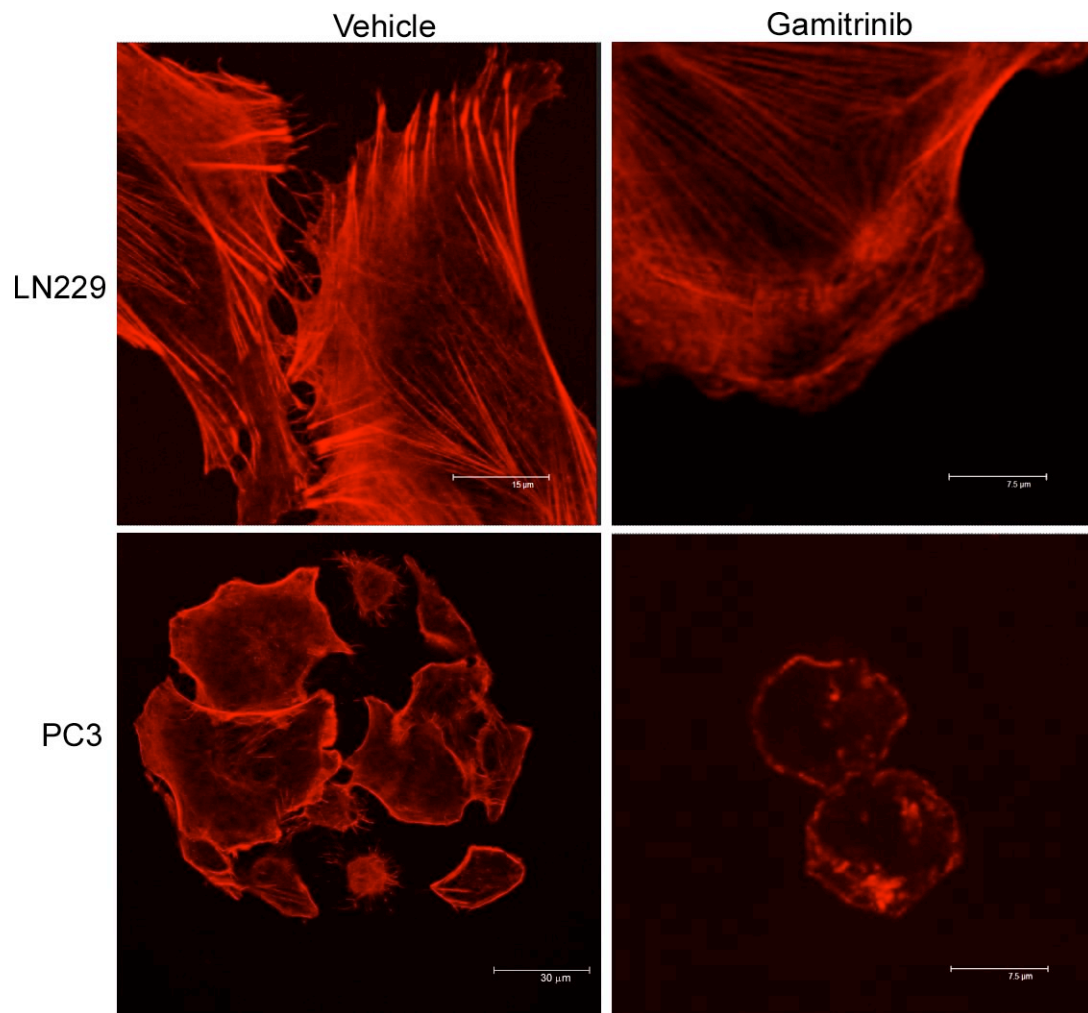
² Seven cases could not be evaluated

³ For two AdCa cases, cytoplasmic ULK1-S757 could not be evaluated

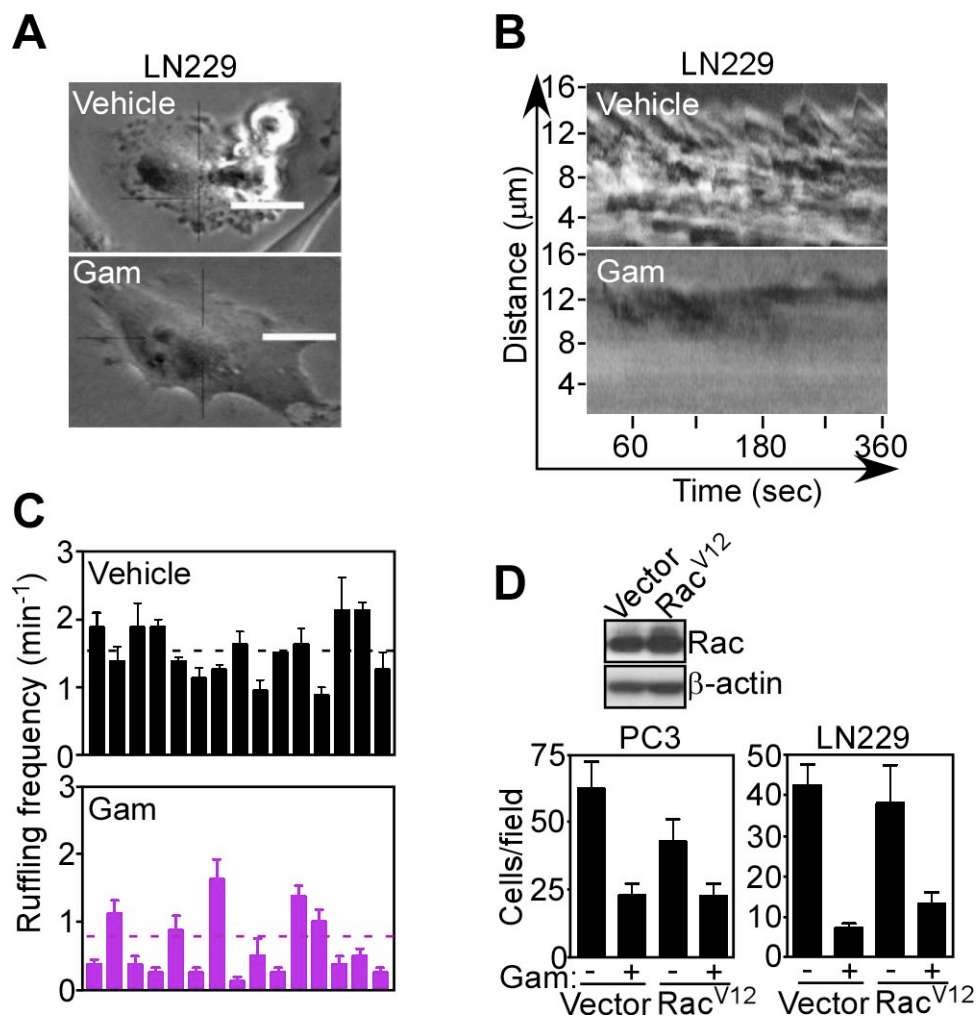
SUPPLEMENTAL FIGURES



Supplemental Figure 1. Control of cell motility by mitochondrial Hsp90s. (**A**, **B**) the indicated tumor cell types were treated with vehicle or Gamitrinib (5 μ M) and analyzed for cell migration (**A**) or invasion (**B**) after 6 or 16 h, respectively. Mean \pm SD (n=3). ***, p<0.0001.

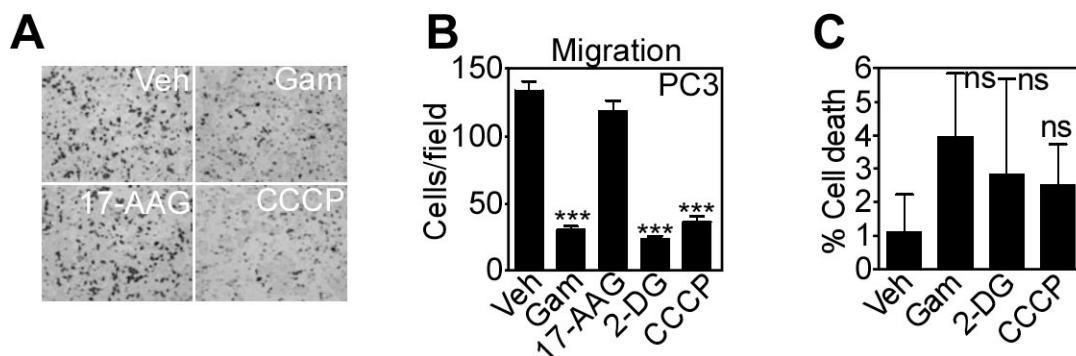


Supplemental Figure 2. Mitochondrial Hsp90 regulation of the actin cytoskeleton. The indicated tumor cell types were treated with vehicle or Gamitrinib (5 μ M), stained with rhodamine-phalloidin and analyzed by confocal microscopy. Magnification, x1000.

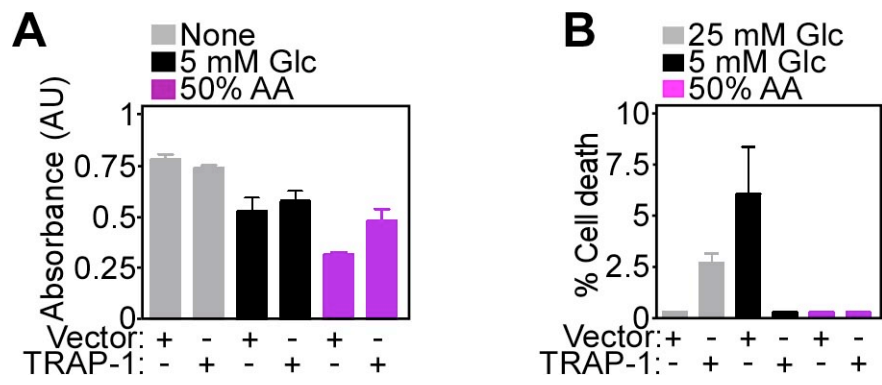


Supplemental Figure 3. Real-time single cell analysis of cytoskeletal dynamics by mitochondrial Hsp90s. **(A)** Still images of time lapse videomicroscopy of individual LN229 cells treated with vehicle or Gamitrinib ($5 \mu\text{M}$). Individual subcellular areas selected for SACED analysis are depicted as vertical and horizontal lines (4 lines per cell). **(B)** Stroboscopic images depicting the kinetics of membrane ruffling (lamellipodia growth and retraction) in vehicle- or Gamitrinib-treated LN229 cells. **(C)** Quantification of membrane ruffling frequency in vehicle- or Gamitrinib-treated LN229 cells. Each bar corresponds to an individual cell. Average values are indicated by dotted lines. **(D)** The indicated tumor cell types were

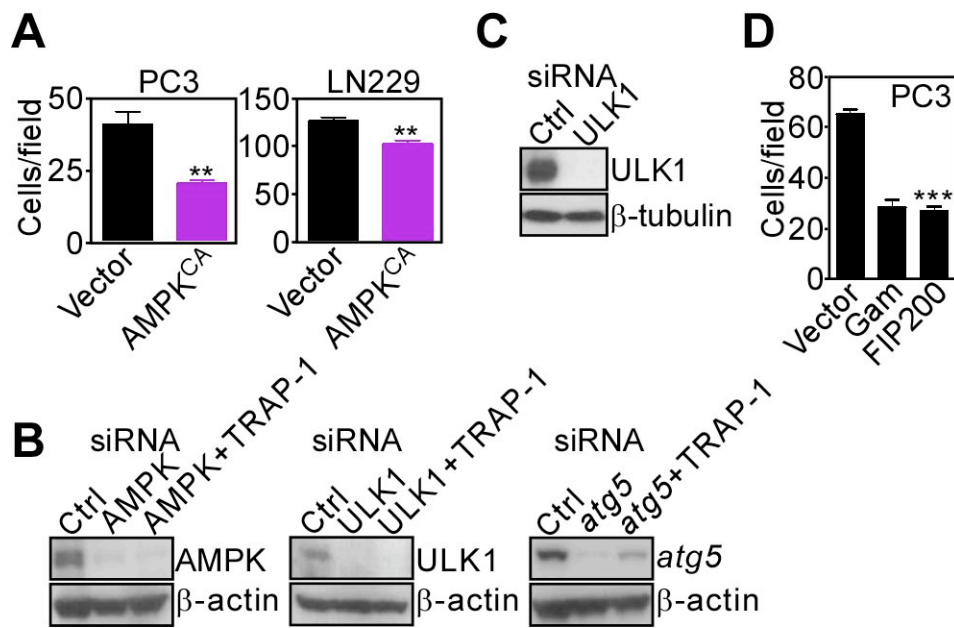
transfected with vector or constitutively active Rac^{V12} mutant cDNA and analyzed for cell invasion with (+) or without (-) Gamitrinib. Mean±SD (n=3).



Supplemental Figure 4. Mitochondrial Hsp90-directed bioenergetics controls tumor cell migration under stress. (**A, B**) PC3 cells treated with Gamitrinib (5 μ M), 17-AAG (5 μ M), 2-DG (25 mM) or CCCP (12.5 μ M) were analyzed for cell migration after 6 h by phase contrast microscopy (**A**), and quantified (**B**). Mean \pm SEM (n=3). ***, p<0.0001. (**C**) PC3 cells were treated as in (**A**) and analyzed for changes in cell viability by Trypan blue exclusion. Mean \pm SEM (n=3); ns, not significant.



Supplemental Figure 5. Mitochondrial Hsp90s-directed bioenergetics under stress conditions. **(A)** NIH3T3 fibroblasts were transfected with vector or TRAP-1 cDNA, maintained in normal growth conditions (None) or suspended in 5 mM glucose (Glc) or 50% concentrations of amino acids (AA), and analyzed for cell viability by MTT. AU, arbitrary units. **(B)** The experimental conditions are as in **(A)**, except that control or TRAP-1 transfectants were analyzed for cell viability by Trypan blue exclusion. Mean \pm SD (n=3).



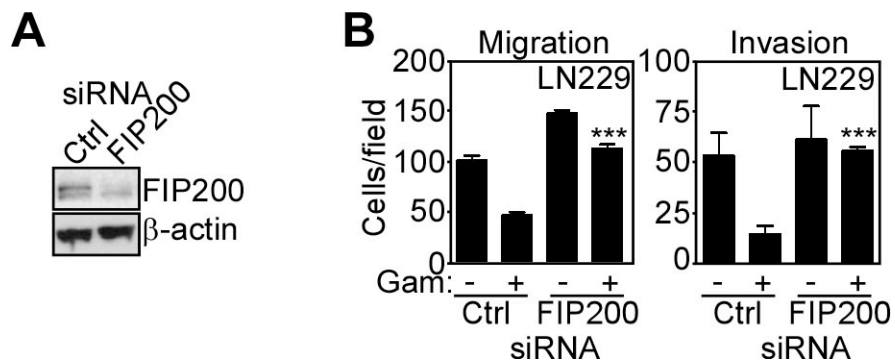
Supplemental Figure 6. ULK1-FIP200 regulation of tumor cell motility. (A)

The indicated tumor cell types were transfected with vector or constitutively active AMPK α 1 cDNA (AMPK^{CA}) and analyzed for cell migration. Mean \pm SD (n=3). **, p<0.001.

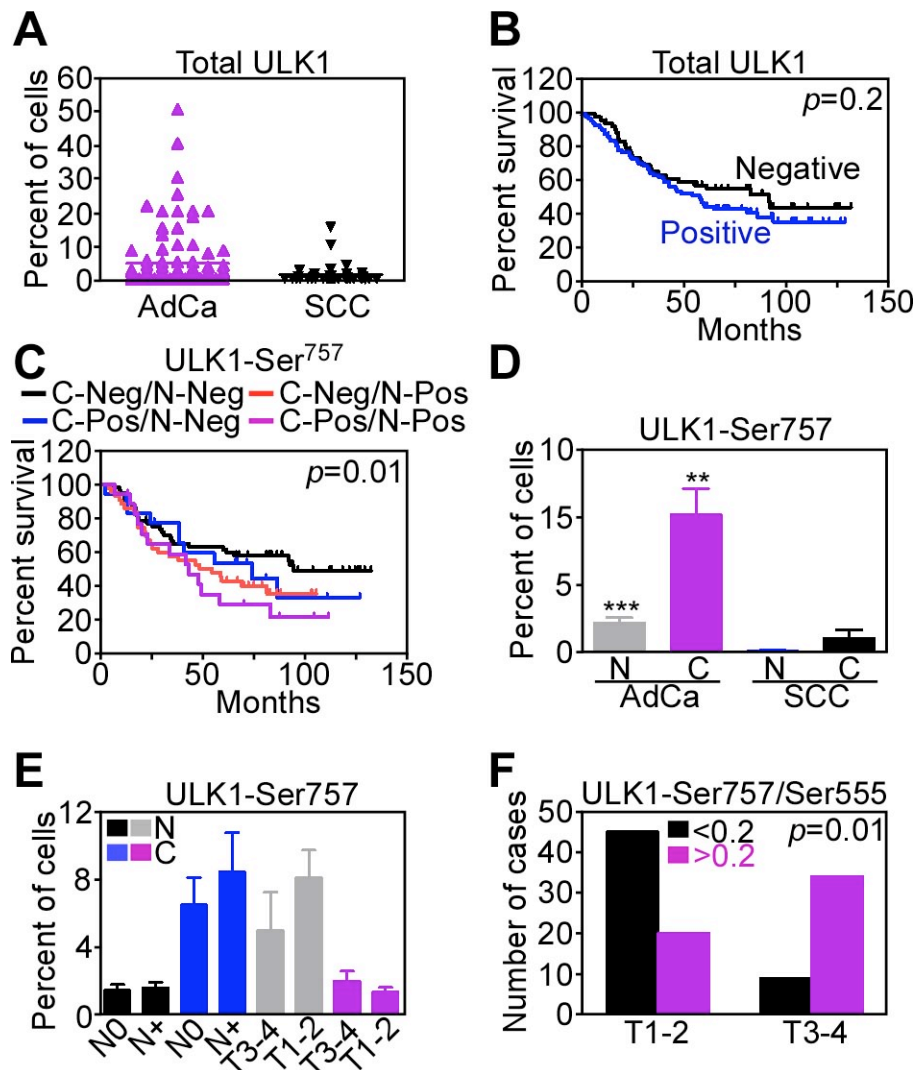
(B) PC3 cells were transfected with control siRNA (Ctrl) or siRNA directed to AMPK, ULK1 or *atg5*, alone or in combination with TRAP-1-directed siRNA, and analyzed by Western blotting.

(C) PC3 cells were transfected with control (Ctrl) or ULK1-directed siRNA, and analyzed by Western.

(D) PC3 cells transfected with vector or FIP200 cDNA were analyzed for cell migration after 6 h. Mean \pm SEM (n=3). ***, p<0.0001.



Supplemental Figure 7. FIP200 regulation of tumor cell motility. (**A**, **B**) PC3 cells were transfected with control (Ctrl) or FIP200-directed siRNA and analyzed by Western blotting (**A**) or cell migration (**B**, *left*) or cell invasion (**B**, *right*) in the presence (+) or absence (-) of Gamitrinib. Mean±SD (n=3). ***, p<0.0001.



Supplemental Figure 8. Differential ULK1 phosphorylation influences disease outcome in NSCLC patients. (A) Expression of total ULK1 protein in the NSCLC patients series analyzed in this study. AdCa, adenocarcinoma; SCC, squamous cell carcinoma. (B) Overall survival of NSCLC patients with positive or negative expression of total ULK1 protein. (C) Overall survival of NSCLC patients according to positive (Pos) or negative (Neg) expression of Ser757-phosphorylated ULK1 in cytoplasm (C) or nuclei (N). (D) Preferential expression of

Ser757-phosphorylated ULK1 in lung AdCa compared to SCC. N, nuclear; C, cytoplasmic. **(E)** Correlation between expression of Ser757-phosphorylated ULK1 and NSCLC stage or lymph node metastasis. N0, no lymph node metastasis; N+, one or more lymph node metastasis; T, tumor size, 1-2 or 3-4. N, nuclear; C, cytoplasmic. **(F)** Correlation between expression of Ser757/Ser555-phosphorylated ULK1 ratio (cutoff, 0.2) and tumor size (T1-2 versus T3-4).

SUPPLEMENTAL REFERENCES

1. Kang, B.H., Plescia, J., Song, H.Y., Meli, M., Colombo, G., Beebe, K., Scroggins, B., Neckers, L., and Altieri, D.C. 2009. Combinatorial drug design targeting multiple cancer signaling networks controlled by mitochondrial Hsp90. *J Clin Invest* 119:454-464.
2. Flaiz, C., Chernoff, J., Ammoun, S., Peterson, J.R., and Hanemann, C.O. 2009. PAK kinase regulates Rac GTPase and is a potential target in human schwannomas. *Exp. Neurol.* 218:137-144.
3. Hinz, B., Alt, W., Johnen, C., Herzog, V., and Kaiser, H.-W. 1999. Quantifying Lamella Dynamics of Cultured Cells by SACED, a New Computer-Assisted Motion Analysis. *Exp. Cell Res.* 251:234-243.
4. Kinoshita, E., Kinoshita-Kikuta, E., and Koike, T. 2009. Separation and detection of large phosphoproteins using Phos-tag SDS-PAGE. *Nat. Protocols* 4:1513-1521.
5. Barberis, M., Pellegrini, C., Cannone, M., Arizzi, C., Coggi, G., and Bosari, S. 2008. Quantitative PCR and HER2 testing in breast cancer: a technical and cost-effectiveness analysis. *Am. J. Clin. Pathol.* 129:563-570.